Proceedings of 2019 IEEE
International Conference on Mechatronics and Automation
August 4 - 7, Tianjin, China

Guidewire Tracking based on Visual Algorithm for Endovascular Interventional Robotic System

Peng Shi[1], Shuxiang Guo[1,2*], Linshuai Zhang[1]
Xiaoliang Jin[1], Dapeng Song[1] and Weihao Wang[1]

[1]*Department of Intelligent Mechanical Systems Engineering*
Faculty of Engineering and Design
Kagawa University
Hayashi-cho, Takamatsu, 761-0396, Japan
s19d503@stu.kagawa-u.ac.jp

[2]*Key Laboratory of Convergence Medical Engineering System and Healthcare Technology, The Ministry of Industry and Information Technology, School of Life Science*
Beijing Institute of Technology
Haidian District, Beijing 100081 China
**corresponding author: guo@eng.kagawa-u.ac.jp*

***Abstract* – During the Minimally invasive vascular intervention surgery, deformable guidewire tracking is still a challenging task due to background clutter of the image and the complex motion of the target. However, existing researches about guidewire tracking for robot-assisted endovascular catheterization system are still limited. In this paper, scale-adaptive mean-shift method is adopted in endovascular interventional robotic system to detect the position of the guidewire tip. To evaluate the performance of this algorithm in guidewire tracking, two interventional experiment using the rigid model of cerebral vascular were designed. The experimental results show that the ratio of frames with the center location error less than 5 pixels is 97.6% in these two tasks, and the average processing speed for each frame is 1.24ms. The result shows that this algorithm with high precision and real-time has the potential to apply in endovascular interventional robotic system.**

Index Terms* – *Guidewire tracking; scale-adaptive mean-shift; endovascular interventional robotic system

I. INTRODUCTION

Vascular interventional surgery (VIS) is a surgical technique that limit the size of incisions and so lessen wound healing time, associated pain and risk of infection [1]. During the procedure, the surgeon inserts the catheter in the femoral artery. Then, under fluorescent image, the surgeon manipulates the guidewire to guide the catheter move to the lesions and inject drugs or put therapeutic device (stent balloon) [2]. For the VIS, accurate positioning of the guidewire with respect to the vasculature is a prerequisite for a successful procedure [3]. However, due to the narrowness of the blood vessels and the complexity of the vasculature, guidewire tracking is difficult, especially during procedure [4]. This result prolongs the operation time, and long-term exposure of doctors and patients to radiation will affect their health.

There have been many studies on the tracking of catheters, guidewires and other endovascular tools through different means so far. Electromagnetic (EM) trackers, which are placed motion-sensor on the tip of the catheter with high spatial resolution, high sensitivity, and low noise, have been used by many researchers for tracking the tip of guidewire. A 3D EM tracking system in conjunction with fluoroscopy and angiography has shown that the use of this system has potential to apply in complicated endovascular procedures and reduce the radiation exposure [5]. Based on fusion framework, the information from customized catheter with multi-EM sensors have been combined to estimate guidewire shape and position within the vasculature. This provides continuous guidewire position information without using contrast agents and fluoroscopy frequently [6].

Visual-based tracker use image processing techniques in X-ray fluoroscopy or MR image to visualize the current position of endovascular tools inside the patient vasculature in real time. Correlation filter algorithm [7], machine learning algorithms [8], or combinations of different algorithms [9] have been achieved high tracking accuracy. These algorithms establish the model of guidewire and update this model online using machine learning algorithm to obtain the robust tracking performance. In addition, several MR compatibility tools for tracing have been developed, such as using the negative small paramagnetic rings or magnetite mixtures, resonant radiofrequency (RF) coils, Hall probes, and Faraday sensors [10].

Via current studies have achieved acceptable accuracy and real-time performance, these tracking methods still have several limitations. Due to the soft and fine structure of the guidewire, sensor used in tracking would difficult to apply to conventional catheters. visual-based tracking methods focus on describing catheter model, due to the special structure of the catheter increases the difficulties and cannot meet accuracy, robustness, and real-time requirements. As a result, guidewire tracking is still a clinical challenge in endovascular intervention surgery.

In this paper, visual-based scale-adaptive mean-shift algorithm was adopted to track the guidewire to reduce the X-ray exposure and improve surgical safety [11]. Surgeon can mark the object of interest (guidewire, catheter and tools) during the procedure, the algorithm will establish the target model in real time. In the next image frame, through the established target model, this algorithm can iterate the new position of the target quickly. Two interventional tasks using the vascular phantom with different path were designed to evaluate the tracking accuracy and real-time performance of the algorithm.

The remainder of this paper is organized as follows. The experiment platform was introduced in section II. The detail of

978-1-7281-1697-6/19/$31.00 ©2019 IEEE

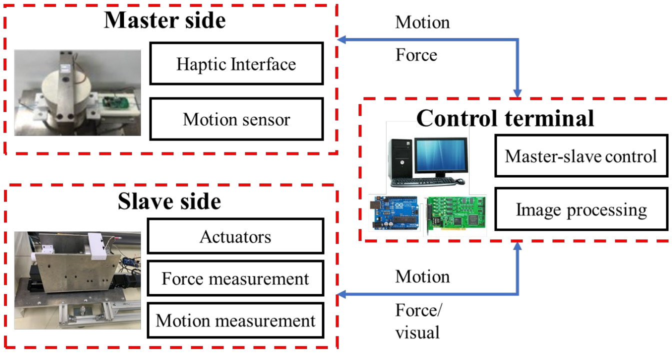

Fig. 1 Master-slave interventional robotic system

scale-adaptive mean-shift method was given in section III. We used two intervention tasks with different path to evaluate the performance of the algorithm. Section IV present the experimental results. Finally, section V concludes this paper.

II. EXPERIMENT PLATFORM

Fig.1 presents the block diagram of the master-slave interventional robotic system which designed by our research team [12]-[16].

The master device measures the translation and rotation of the catheter and provide the force feedback from slave side to the manipulators. The two degrees of freedom linear and rotational motion of the catheter for master side is measured by the laser mouse's image sensor. Haptic interfaces based on magnetorheological fluid (MRF) provides the surgeon with real force feedback to improve the safety of the procedure.

The slave device is used to manipulate the patient catheter movement, push-pull and rotation. The clamping mechanism is controlled by a relay which can operate the spring mechanism to clamp the catheter with different size. The movement of the catheter (push-pull and rotation) is controlled by two stepping motors through the ball screw and pulley mechanism. Load cell was used in slave side to measure the proximal force during the surgery.

The control terminal can process the motion signal from the master side, the force feedback signal from the slave side and the visual feedback signal. The visual-based tracking method can be used in control terminal to provide guidewire positioning for interventionalists. In addition, visualized data will be provided to the surgeon to improve the safety of the operation.

III. SCALE-ADAPTIVE MEAN-SHIFT ALGORITHM

A. *Standard Mean-shift Tracking Method*

According to classical mean-shift method, the target is described as a multivariate kernel density estimate in origin-located feature space

$$\mathrm{q}=\{q_u\}_{u=1\ldots m} \qquad \sum_{u=1}^{m} q_u=1 \tag{1}$$

In the next frame, the target candidate at location y is modelled as

$$\mathrm{p(y)}=\{p_u(\mathrm{y})\}_{u=1\ldots m} \qquad \sum_{u=1}^{m} p_u=1 \tag{2}$$

Let x_i be the pixel locations and $\{\mathrm{x}_i^*\}_{i=1\ldots n}$ be the pixel locations of the target model centred at zero, where n be the number of pixels. The grayscale-image space of the selected area is evenly divided, and then a grayscale histogram composed of m equal regions is obtained. The probability of the feature $u\in\{1,\ldots,m\}$ is estimated by the target histogram as

$$q_u=C\sum_{i=1}^{n} k(\|\mathrm{x}_i^*\|^2)\delta[b(\mathrm{x}_i^*)-u] \tag{3}$$

where $k(x)$ is kernel function. $b(\mathrm{x}_i^*)$ denote the histogram interval of the pixel located in x_i^* and u is the index of color histogram. δ is the *Kronecker* function, which is used to detect whether the gray value at the pixel x_i^* in the target area belongs to the color unit u in the histogram. C is the normalization constant so as $\sum_{u=1}^{m} q_u=1$.

In the current frame, the center position y of the target candidate is obtained by search area located at center position y_0 in last frame. The pixel locations of search area are represented by $\{\mathrm{x}_i\}_{i=1\ldots n_h}$, where the n_h be the pixel number of search area. Using the same kernel function $k(x)$, the probability of the target candidate is

$$p_u(\mathrm{y})=C_h\sum_{i=1}^{n_h} k\left(\left\|\frac{\mathrm{y}-\mathrm{x}_i}{h}\right\|^2\right)\delta[b(\mathrm{x}_i)-u] \tag{4}$$

where h is scale parameter, C_h is a normalization constant. The similarity function is used to measure the difference between the target model $\{q_u\}_{u=1\ldots m}$ and the target candidate $\{p_u(\mathrm{y})\}_{u=1\ldots m}$. Using the Hellinger distance to calculate the similarity, which is given by

$$H(\mathrm{p(y)},\mathrm{q})=\sqrt{1-\rho[\mathrm{p(y)},\mathrm{q}]} \tag{5}$$

where

$$\rho[\mathrm{p(y)},\mathrm{q}]=\sum_{u=1}^{m}\sqrt{p_u(\mathrm{y})q_u} \tag{6}$$

is the Bhattacharyya coefficient between q and p(y). Maximizing the Bhattacharyya coefficient $\rho[\mathrm{p(y)},\mathrm{q}]$ is equivalent to minimizing the Hellinger distance. The new position of the target from the y_0 in the last frame to the y_1 in current frame is iteratively moved via maximizing similarity of target model and target candidate.

$$\mathrm{y}_1=\frac{\sum_{i=1}^{n_h}\mathrm{x}_i w_i g\left(\left\|\frac{\mathrm{y}_0-\mathrm{x}_i}{h}\right\|^2\right)}{\sum_{i=1}^{n_h} w_i g\left(\left\|\frac{\mathrm{y}_0-\mathrm{x}_i}{h}\right\|^2\right)} \tag{7}$$

where

$$w_i = \sum_{u=1}^{m} \sqrt{\frac{q_u}{p_u(\mathrm{y}_0)}} \delta[b(\mathrm{x}_i) - u] \tag{8}$$

and $g(x) = -k'(x)$ is the derivative of $k(x)$.

B. Scale Estimation

Let us assume that the scale change of the target in successive frames is isotropic. Let $y = (y^1, y^2)^T$, $x_i = (x_i^1, x_i^2)^T$ denote pixel locations and N be the pixel number in the image. The target is described in the image by an ellipsoidal region $\frac{(x_i^{*1})^2}{a^2} + \frac{(x_i^{*2})^2}{b^2} < 1$ with an isotropic kernel $k(x)$, restricted by a condition $k(x) = 0$ for $x \geq 1$. The probability of the feature $u \in \{1, ..., m\}$ is estimated by the target histogram as

$$q_u = C \sum_{i=1}^{N} k\left(\frac{(x_i^{*1})^2}{a^2} + \frac{(x_i^{*2})^2}{b^2} \right) \delta[b(\mathrm{x}_i) - u] \tag{9}$$

where C is a normalization constant. Let $\{\mathrm{x}_i\}_{i=1 \ldots N}$ be the pixel locations of the target candidate in the current frame Using the same kernel function $k(x)$, the probability of the feature $u \in \{1, ..., m\}$ in the target candidate is

$$p_u(\mathrm{y}, h) = C_h \sum_{i=1}^{N} k\left(\frac{(y^1 - x_i^1)^2}{a^2 h^2} + \frac{(y^2 - x_i^2)^2}{b^2 h^2} \right) \delta[b(\mathrm{x}_i) - u] \tag{10}$$

where

$$C_h = \frac{1}{\sum_{i=1}^{N} k\left(\frac{(y^1 - x_i^1)^2}{a^2 h^2} + \frac{(y^2 - x_i^2)^2}{b^2 h^2} \right)} \tag{11}$$

The parameter h is the scale of the target candidate. Let n_1 be the pixel number of the target model, and n_h be the pixel number of the target candidate with a scale h in the ellipsoidal region; then $n_h = h^2 n_1$. According to the definition of Riemann integral, we obtain:

$$\begin{aligned} &\sum_{i=1}^{N} k\left(\frac{(x_i^1)^2}{a^2 h^2} + \frac{(x_i^2)^2}{b^2 h^2} \right) \frac{\pi a b h^2}{n_h} \\ &\approx \iint_{\left\{ \frac{(x_i^1)^2}{a^2 h^2} + \frac{(x_i^2)^2}{b^2 h^2} < 1 \right\}} k\left(\frac{(x_i^1)^2}{a^2 h^2} + \frac{(x_i^2)^2}{b^2 h^2} \right) dx^1 dx^2 \\ &= h^2 ab \iint_{\|x\| < 1} k(\|\mathrm{x}\|^2)\, d\mathrm{x} \end{aligned} \tag{12}$$

Thus $C_h \approx C \frac{1}{h^2}$, For any two values h_0, h_1, we obtain $C_{h_1} \approx C_{h_0} \frac{h_0^2}{h_1^2}$.

The similarity between the target model and the target candidate is calculated by the Bhattacharyya parameter. Using the approximations above for C_h we get

$$\begin{aligned} &\rho[\mathrm{p}(\mathrm{y}, h), \mathrm{q}] \approx \rho[\mathrm{y}, h] \\ &= \sum_{u=1}^{m} \sqrt{C_{h_0} \frac{h_0^2}{h^2} \sum_{i=1}^{N} k\left(\frac{(y^1 - x_i^1)^2}{a^2 h^2} + \frac{(y^2 - x_i^2)^2}{b^2 h^2} \right) \delta[b(\mathrm{x}_i) - u] q_u} \end{aligned} \tag{13}$$

Thus, to maximized $\rho[\mathrm{p}(\mathrm{y}, h), \mathrm{q}]$, center position y_0 in last frame iteratively move to the new location y_1, changing its scale to h_1.

Let us denote

$$w_i = \sum_{u=1}^{m} \sqrt{\frac{q_u}{p_u(y_0, h_0)}} \delta[b(x_i) - u] \tag{14}$$

$$G = \sum_{i=1}^{N} w_i g\left(\frac{(y_0^1 - x_i^1)^2}{a^2 h_0^2} + \frac{(y_0^2 - x_i^2)^2}{b^2 h_0^2} \right) \tag{15}$$

and

$$m_k(y_0, h_0) = \frac{\sum_{i=1}^{N} x_i w_i g\left(\frac{(y_0^1 - x_i^1)^2}{a^2 h_0^2} + \frac{(y_0^2 - x_i^2)^2}{b^2 h_0^2} \right)}{G} - y_0 \tag{16}$$

where $m_k(y_0, h_0) = (m_k^1(y_0, h_0), m_k^2(y_0, h_0))^T$. Then we get

$$\frac{\partial \rho[\mathrm{y}, h]}{\partial y^1}(\mathrm{y}_0, h_0) = \frac{C_{h_0}}{a^2 (h_0)^2} \cdot G \cdot m_k^1(\mathrm{y}_0, h_0) \tag{17}$$

$$\frac{\partial \rho[\mathrm{y}, h]}{\partial y^2}(\mathrm{y}_0, h_0) = \frac{C_{h_0}}{b^2 (h_0)^2} \cdot G \cdot m_k^2(\mathrm{y}_0, h_0) \tag{18}$$

and

$$\begin{aligned} \frac{\partial \rho[\mathrm{y}, h]}{\partial h}(\mathrm{y}_0, h_0) = \frac{C_{h_0}}{(h_0)^2} \cdot G \cdot \Bigg[& \frac{1}{h_0} \frac{\sum_{i=1}^{N} w_i \left(\frac{(y_0^1 - x_i^1)^2}{a^2} + \frac{(y_0^2 - x_i^2)^2}{b^2} \right) g\left(\frac{(y_0^1 - x_i^1)^2}{a^2 h_0^2} + \frac{(y_0^2 - x_i^2)^2}{b^2 h_0^2} \right)}{G} \\ & - h_0 \frac{\sum_{i=1}^{N} w_i k\left(\frac{(y_0^1 - x_i^1)^2}{a^2 h_0^2} + \frac{(y_0^2 - x_i^2)^2}{b^2 h_0^2} \right)}{G} \Bigg] \end{aligned} \tag{19}$$

Finally, the new position y and new scale h is obtained by

$$y_1^1 = \frac{1}{a^2} m_k^1(y_0, h_0) + y_0^1, y_1^2 = \frac{1}{b^2} m_k^2(y_0, h_0) + y_0^2 \tag{20}$$

$$\begin{aligned} h_1 = &\left[1 - \frac{\sum_{i=1}^{N} w_i k\left(\frac{(y_0^1 - x_i^1)^2}{a^2 h_0^2} + \frac{(y_0^2 - x_i^2)^2}{b^2 h_0^2} \right)}{G} \right] h_0 \\ &+ \frac{1}{h_0} \frac{\sum_{i=1}^{N} w_i \cdot \left(\frac{(y_0^1 - x_i^1)^2}{a^2} + \frac{(y_0^2 - x_i^2)^2}{b^2} \right) \cdot g\left(\frac{(y_0^1 - x_i^1)^2}{a^2 h_0^2} + \frac{(y_0^2 - x_i^2)^2}{b^2 h_0^2} \right)}{G} \end{aligned} \tag{21}$$

C. Mean-shift with scale estimation

To prevent the tracking error generated by scale estimation, we check the consistency of forward-backward scale change. The forward-backward check compares the estimated scale from frame $t-1$ to t and t to $t-1$ .This validation ensure that the target scale will not grow indefinitely and enable the tracker to recover from erroneous estimate. The algorithm mainly consists of the following steps.

Input: Target model q, initialization position y_0 and initialization target size s_0.

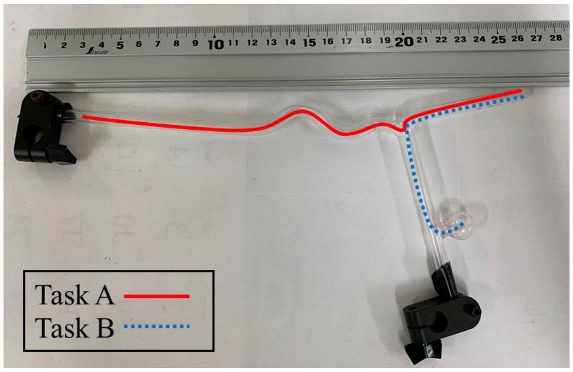

Fig. 2 Two intervention tasks using a rigid model of cerebral vascular

Output: Position y_t and scale h_t.

For each frame $t \in \{1,...,n\}$:

1) Compute $p_u(y_{t-1}, h_{t-1})$ using Eq. (10).

2) Update position y_t according to Eq. (20).

3) Update scale h_t according to Ep. (21).

4) If $\|y_t - y_{t-1}\|^2 \le \varepsilon$ or the maximum step of iteration $t > maxIter$, go to the next step 5), else go to the step 1).

5) If $|log(h_t)| > \Theta_s$, then the target scale changes, go to the next step 6) to perform the forward-backward scale check, else the scale estimation is $s_t = (1-\gamma)s_{t-1} + \gamma h s_{t-1}$.

6) Use the step 1) to 4) to compute the backward scale h_{back} from frame t to $t-1$. If $|log(h_t * h_{back})| > \Theta_c$, then the forward-backward scale changes are inconsistent, the scale estimation is $s_t = (1-\alpha-\beta)s_{t-1} + \alpha s_{default} + \beta h_t s_{t-1}$, where $\alpha = c_1\left(\frac{s_{default}}{s_{t-1}}\right)$.

The above algorithm was compiled using visual studio 2017 with OpenCV 4.0 library and tested on DELL G5 5587 (Intel Core i7-8750H CPU, 16G RAM). The parameter values in the algorithm are as follows: $\varepsilon = 0.1$, $maxIter = 15$, $\Theta_s = 0.05$, $\Theta_c = 0.1$, $c_1 = 0.1$, $\beta_1 = 0.1$, $\gamma_1 = 0.3$, where $s_{default}$ is the scale from first frame initialization.

IV. Experimental Results

We designed two intervention tasks using a rigid model of cerebral vascular with different paths to evaluate the performance of the tracking method running on the endovascular intervention system. The length of vascular model is about 25cm, which include one vascular intersection, one hemangioma and four blood vessels bending. Catheter move from right to left, and the path are shown by Fig.2. We use the master-slave interventional robotic system designed by our lab to manipulate the catheter. The average speed of catheter movement in these tasks is 0.75cm/s.

In the beginning of the task, we mark the catheter tip to be the interest box, and the method will track this area on the following sequence. For each frame, the algorithm will track the target location and write the coordinates of the target into

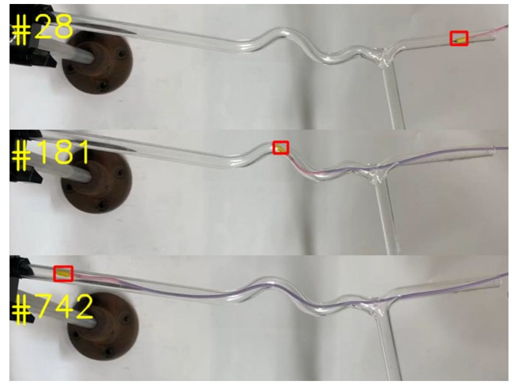

Fig. 3 Tracking performance in task A

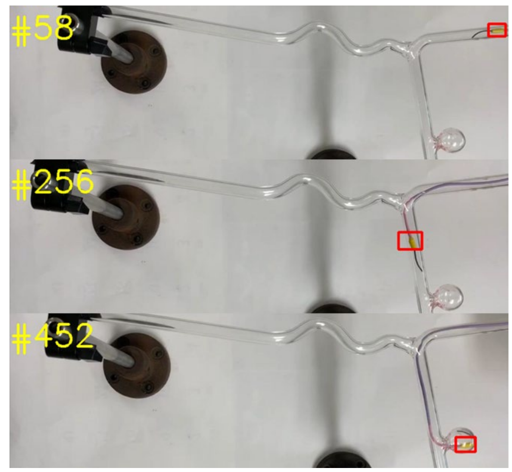

Fig. 4 Tracking performance in task B

the txt file. In addition, we manually mark the catheter tip to be the ground truth box for each frame of the mission. This ground truth box file can be used to verify the performance of the algorithm.

The mainly challenge in the task is that tracking error caused by blood vessel contour to guidewire interference and deformation due to contact between the catheter and the vessel wall. In addition, blurring due to catheter movement is also likely to cause tracking failure. Fig.3 and Fig.4 shows part of tracking performance in task A and B. We mark the catheter tip at the first frame, and during the following sequence, to face the deformation and the background clutter, the adaptive scale mean-shift algorithm can track it at the real time.

We use the success and precision rate for quantitative analysis, and the results are shown by success plots and precision plots [17]. Precision plot is one of evaluation metric using center location error, which is defined as the average Euclidean distance between the center locations of the bounding box (created by tracker) and the manually labeled ground truth box. In Fig.5, the x axes is the center location error, and the y axes is the ratio of number of frames whose location error less than threshold. Success plot is another evaluation metric using bounding box overlap. Let denote r_t be the tracked bounding box and r_a be the ground truth box,

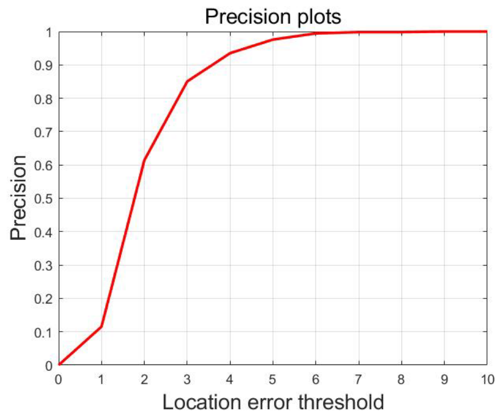

Fig. 5 Algorithm performance described by precision plots

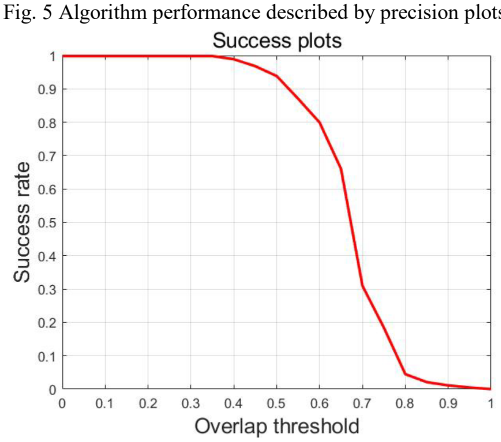

Fig. 6 Algorithm performance described by success plots

the overlap is counted by

$$S = \frac{|r_t \cap r_a|}{|r_t \cup r_a|} \tag{22}$$

where $\cap$ and $\cup$ represent the intersection and union of two boxes respectively, and $|\bullet|$ is the number of pixels in the box. In Fig.6, the x axes is the overlap threshold, and the y axes is the ratio of number of frames whose overlap large than threshold.

We use center location error less than 5 pixels and overlap large than 50% as a standard for evaluating the performance of the tracking method. As shown in the Fig.11, the proportion of frames with the center location error less than 5 pixels is 97.60%, and the proportion of frames with the overlap large than 50% is 93.84%. In addition, the average processing speed for each frame is 1.24ms.

V. Conclusion

In this paper, the visual-based tracking method has been utilized to assist the operator in guidewire positioning. Experimental results illustrated that this method with high precision and real-time has the potential to apply in endovascular interventional system. However, guidewire tracking will face low resolution and background clutters in fluorescent images during actual surgical procedures. In the next study, using this method at *in vitro* experiment should be taken into account.

Acknowledgment

This research is partly supported by National High-tech Research and Development Program (863 Program) of China (No.2015AA043202), and SPS KAKENHI Grant Number 15 K2120.

References

[1] S. Guo, Y. Song, X. Yin, L. Zhang, Takashi Tamiya, Hideyuki Hirata, Hidenori Ishihara, “A Novel Robot-Assisted Endovascular Catheterization System with Haptic Force Feedback”, *The IEEE Transactions on Robotics,* DOI: 10.1109/TRO.2019.2896763, 2019.

[2] X. Yin, S. Guo, Y. Song, “Magnetorheological fluids actuated haptic-based teleoperated catheter operating system”, *Micromachines,* vol.9, no.9, DOI: 10.3390/mi9090465, 2018.

[3] X. Zhou, G. Bian, X. Xie, and Z. Hou, "An Interventionalist-Behavior-Based Data Fusion Framework for Guidewire Tracking in Percutaneous Coronary Intervention," *IEEE Transactions on Systems, Man, and Cybernetics: Systems,* pp. 1-14, 2018.

[4] M. Hoffmann et al., "Electrophysiology Catheter Detection and Reconstruction From Two Views in Fluoroscopic Images," *IEEE Transactions on Medical Imaging,* vol. 35, no. 2, pp. 567-579, 2016.

[5] A. M. Franz, T. Haidegger, W. Birkfellner, K. Cleary, T. M. Peters, and L. Maier-Hein, "Electromagnetic Tracking in Medicine—A Review of Technology, Validation, and Applications," *IEEE Transactions on Medical Imaging,* vol. 33, no. 8, pp. 1702-1725, 2014.

[6] C. Shi et al., "Shape Sensing Techniques for Continuum Robots in Minimally Invasive Surgery: A Survey," *IEEE Transactions on Biomedical Engineering,* vol. 64, no. 8, pp. 1665-1678, 2017.

[7] P. Chang et al., "Robust Catheter and Guidewire Tracking Using B-Spline Tube Model and Pixel-Wise Posteriors," *IEEE Robotics and Automation Letters,* vol. 1, no. 1, pp. 303-308, 2016.

[8] A. Vandini et al., "Robust guidewire tracking under large deformations combining segment-like features (SEGlets)," *Medical image analysis,* vol. 38, pp. 150-164, 2017.

[9] R. C. Jackson, R. Yuan, D. Chow, W. S. Newman, and M. C. Çavuşoğlu, "Real-Time Visual Tracking of Dynamic Surgical Suture Threads," *IEEE Transactions on Automation Science and Engineering,* vol. 15, no. 3, pp. 1078-1090, 2018.

[10] A. Ataollahi et al., "Three-Degree-of-Freedom MR-Compatible Multisegment Cardiac Catheter Steering Mechanism," *IEEE Transactions on Biomedical Engineering,* vol. 63, no. 11, pp. 2425-2435, 2016.

[11] T. Vojir, J. Noskova, and J. Matas, "Robust scale-adaptive mean-shift for tracking," *Pattern Recognition Letters,* vol. 49, pp. 250-258, 2014.

[12] X. Yin, S. Guo, N. Xiao, T. Tamiya, H. Hirata, and H. Ishihara, "Safety Operation Consciousness Realization of a MR Fluids-Based Novel Haptic Interface for Teleoperated Catheter Minimally Invasive Neurosurgery," *IEEE/ASME Transactions on Mechatronics,* vol. 21, no. 2, pp. 1043-1054, 2016.

[13] J. Guo, S. Guo, “A Marker-based Contactless Catheter-sensing Method to Detect Surgeons' Operations for Catheterization Training Systems”, *Biomedical Microdevices,* vol.20, no.3, DOI: 10.1007/s10544-018-0321-5, 2018.

[14] L. Zhang et al., "Performance evaluation of a strain-gauge force sensor for a haptic robot-assisted catheter operating system," *Microsystem Technologies,* vol. 23, no. 10, pp. 5041-5050, 2017.

[15] X. Bao, S. Guo, N. Xiao, Y. Li, L. Shi, “Compensatory force measurement and multimodal force feedback for remote-controlled vascular interventional robot”, *Biomedical Microdevices,* vol.20, no.3, DOI: 10.1007/s10544-018-0318-0, 2018.

[16] C. Zhang, S. Guo, N. Xiao, J. Wu, Y. Li, Y. Jiang, “Transverse Microvibration-based Guide Wire Drag Reduction Evaluation for Vascular Interventional Application”, Biomedical Microdevices, Vol.20, No.3, DOI: 10.1007/s10544-018-0315-3, 2018.

[17] Y. Wu, J. Lim, and M.-H. Yang, "Online object tracking: A benchmark," *in Proceedings of the IEEE conference on computer vision and pattern recognition,* pp. 2411-2418, 2013.